

The Benchmark Mode $\Omega_c \rightarrow \Omega^- \pi^+$ and Its Related Processes

Shuge Zeng, Fanrong Xu,^{*} and Yu Gu

Department of Physics, College of Physics & Optoelectronic Engineering,

Jinan University, Guangzhou 510632, P.R. China

Abstract

The benchmark mode $\Omega_c^0 \rightarrow \Omega^- \pi^+$, which receives purely factorization contribution, is of great importance among all the decay channels of Ω_c^0 decays. In this work, within the framework of non-relativistic quark model (NRQM), we calculate all the 6 baryon transition form factors involving $\frac{1}{2}^+ \rightarrow \frac{3}{2}^+$ decays. The absolute branching fractions of non-leptonic decays $\Omega_c^0 \rightarrow \Omega^- \pi^+$, $\Omega_c^0 \rightarrow \Omega^- \rho^+$ and $\Omega_c^0 \rightarrow \Xi^- \pi^+$ as well as semi-leptonic decays $\Omega_c^0 \rightarrow \Omega^- \ell^+ \nu_\ell$ ($\ell = e, \mu$) are calculated although they cannot be measured directly by current experiment. Based on the prediction $\mathcal{B}(\Omega_c^0 \rightarrow \Omega^- \pi^+) = (3.43 \pm 0.48)\%$ in our work, we further predict the ratios between interested modes and the benchmark mode, giving $R(\Xi^- \pi^+) = 0.16 \pm 0.06$, $R(\Omega^- \rho^+) = 5.33 \pm 0.94$, $R(\Omega^- e^+ \nu_e) = 1.18 \pm 0.22$ and $R(\Omega^- \mu^+ \nu_\mu) = 1.11 \pm 0.20$. The predictions on $\Omega_c^0 \rightarrow \Xi^- \pi^+$ and $\Omega_c^0 \rightarrow \Omega^- e^+ \nu$ agree well with recent measured ratios reported by LHCb in 2023 and ALICE in 2024, respectively.

arXiv:2406.02097v2 [hep-ph] 9 Feb 2025

^{*} Electronic address: fanrongxu@jnu.edu.cn

I. INTRODUCTION

Significant experimental progress has been made in the study of charmed baryon decays in recent years. For the anti-triplet singly charmed baryons Λ_c and $\Xi_c^{0,-}$, substantial experimental data has been accumulated since the measurements of their benchmark decay modes $\Lambda_c \rightarrow pK^-\pi^+$ [1] [2] and $\Xi_c^0 \rightarrow \Xi^-\pi^+$ [3]. As the lightest member of the singly charmed baryon sextet, the Ω_c baryon primarily decays via weak processes. Although its benchmark mode $\Omega_c^0 \rightarrow \Omega^-\pi^+$ has not yet been measured, a relative ratio to this benchmark mode, defined as

$$R(X) = \frac{\mathcal{B}(\Omega_c^0 \rightarrow X)}{\mathcal{B}(\Omega_c^0 \rightarrow \Omega^-\pi^+)}, \quad (1)$$

is experimentally less challenging to determine. By measuring $R(X)$, information related to Ω_c can still be indirectly extracted. Recent measurements have provided results such as:

$$\begin{aligned} \text{LHCb 2023 [5]} : \quad & 10^2 R(\Omega^- K^+) = 6.08 \pm 0.51 \pm 0.40, \\ & 10^2 R(\Xi^-\pi^+) = 15.81 \pm 0.87 \pm 0.43 \pm 0.16 \\ \text{ALICE 2024 [6]} : \quad & 10^2 R(\Omega^- e^+\nu_e) = 1.12 \pm 0.22 \pm 0.27. \end{aligned} \quad (2)$$

Incorporating previously measured results, Table I summarizes all the experimental progress on Ω_c decays to date.

The recent experimental progress necessitates concurrent theoretical studies on Ω_c decays. To align with the current experimental status, estimating the branching fraction of the benchmark mode is both timely and essential, taking priority over calculating the absolute branching fractions of other modes of interest. The mode $\Omega_c^0 \rightarrow \Omega^-\pi^+$ is particularly noteworthy due to its kinematics and dynamics. Classified as a $\frac{1}{2}^+ \rightarrow \frac{3}{2}^+ + 0^-$ decay, this benchmark mode provides rich kinematic information. Furthermore, it receives contributions only from purely factorizable processes, meaning non-perturbative effects are solely described by baryon transition form factors.

Theoretical studies on Ω_c decays date back to the 1990s [7, 8]. However, there was a lull in theoretical efforts until recent years, when renewed interest was sparked by rapid experimental developments. For recent theoretical studies of Ω_c , various phenomenology methodologies have been applied, including the light-front quark model [9, 10], constituent quark model [11], light-cone sum rules [12], and fit in combination with other techniques [13, 14]. In our previous series of work [15–19], within the framework of the topological diagrammatic assisted pole model, we systematically calculated absolute branching fractions of all $\frac{1}{2}^+ \rightarrow \frac{1}{2}^+ + 0^-$ decays using current algebra combined with the MIT bag model, including decays of Ω_c [24]. However, due to the

TABLE I. A summary of measured $R(X)$ in recent experiments.

Results	ALICE(2024)[6]	LHCb(2023)[5]	Belle(2022)[4]	Belle(2021)[20]	Belle(2017)[21, 22]	CLEO(2002)[23]
$R(\Omega^- e^+ \nu_e)$	$1.12 \pm 0.22 \pm 0.27$			$1.98 \pm 0.13 \pm 0.08$		2.439 ± 1.154
$R(\Omega^- \mu^+ \nu_\mu)$				$1.94 \pm 0.18 \pm 0.10$		
$10^2 R(\Xi^- \pi^+)$		$15.81 \pm 0.97 \pm 0.16$	$25.3 \pm 5.2 \pm 3.0$			
$10^2 R(\Omega^- K^+)$		$6.08 \pm 0.51 \pm 0.40$	< 29			
$10^2 R(\Xi^- K^+)$			< 7			
$R(\Omega^- \rho^+)$					> 1.3	

absence of a benchmark mode calculation, our predictions related to Ω_c could not be directly compared with current experimental measurements. In this work, we aim to bridge this gap by incorporating the reference mode and other related channels within the non-relativistic quark model (NRQM). The choice of NRQM is particularly reasonable for studying charmed baryon decays due to the relatively low momentum carried by the decay products. A previous theoretical calculation within NRQM for doubly charmed baryon decays also provided predictions in agreement well with experimental results [25]. Therefore, by consistently applying NRQM to all related modes of Ω_c decays, the reliability of our predictions are expected to be enhanced.

The structure of this paper is organized as follows: Section II begins with a revision of the kinematics associated with non-leptonic and semi-leptonic decays involving $\frac{1}{2}^+ \rightarrow \frac{3}{2}^+$. In Section III, we derive the analytical expressions for form factors within the non-relativistic constituent quark model. Section IV presents numerical analyses of these form factors, calculates the branching fractions for the benchmark mode, and explores other related non-leptonic and semi-leptonic decays, including their relative ratios. Conclusions are drawn in Section V. The appendices provide additional support. Appendix A discusses different conventions and their interrelations, while Appendix B details the calculation of form factors within the non-relativistic quark model.

II. KINEMATICS

The benchmark mode $\Omega_c^0 \rightarrow \Omega^- \pi^+$ is categorized as a $\frac{1}{2}^+ \rightarrow \frac{3}{2}^+ + 0^-$ process, with particular focus on the decuplet baryon $\frac{3}{2}^+$. In this section, we first derive the general kinematics for two-body non-leptonic decays, covering final states that include both pseudoscalar and vector mesons. Additionally, we provide generic kinematic formulas for semi-leptonic decays.

A. Non-leptonic decays

The effective Hamiltonian for Cabibbo-favored (CF) processes in Ω_c^0 decay is given by:

$$\mathcal{H}_{\text{eff}} = \frac{G_F}{\sqrt{2}} V_{cs} V_{ud}^* (c_1 O_1 + c_2 O_2) + \text{H.c.} \quad (3)$$

with the four-quark operators:

$$O_1 = (\bar{s}c)(\bar{u}d), \quad O_2 = (\bar{s}d)(\bar{u}c), \quad (4)$$

where $(\bar{q}_1 q_2) = \bar{q}_1 \gamma_\mu (1 - \gamma_5) q_2$. The leading-order Wilson coefficients are $c_1 = 1.346$ and $c_2 = -0.636$ [15]. For convenience, the effective Wilson coefficients $a_1 = c_1 + c_2/N_{\text{eff}}$ and $a_2 = c_2 + c_1/N_{\text{eff}}$ are introduced.

Without delving into the specifics of the dynamics, the decay amplitudes for $\frac{1}{2}^+ \rightarrow \frac{3}{2}^+$ transitions can be parameterized generically as:

$$\begin{aligned} M(\mathcal{B}_i \rightarrow \mathcal{B}_f P) &= i q_\mu \bar{u}_f^\mu(p_f) (C + D \gamma_5) u_i(p_i), \\ M(\mathcal{B}_i \rightarrow \mathcal{B}_f V) &= \bar{u}_f^\nu(p_f) \epsilon^{*\mu} \left[g_{\nu\mu} (C_1 + D_1 \gamma_5) + p_{i\nu} \gamma_\mu (C_2 + D_2 \gamma_5) + p_{i\nu} p_{f\mu} (C_3 + D_3 \gamma_5) \right] u_i(p_i), \end{aligned} \quad (5)$$

for pseudoscalar and vector mesons in the final state, respectively [7]. The final state spin- $\frac{3}{2}$ baryon \mathcal{B}_f is described by the Rarita-Schwinger vector spinor u^μ with momentum p_f , while the initial baryon \mathcal{B}_i is characterized by momentum p_i . Due to its Lorentz structure, more terms appear in the $\frac{1}{2}^+ \rightarrow \frac{3}{2}^+ + 1^+$ transition, hence it is more convenient to use the helicity amplitude framework.

The decay widths can be expressed as

$$\Gamma(\mathcal{B}_i \rightarrow \mathcal{B}_f M) = \frac{p_c}{16\pi m_i^2} H_M, \quad (M = P, V), \quad (6)$$

where

$$\begin{aligned} H_P &= \frac{Q_+ Q_-}{3m_f^2} (Q_+ |C|^2 + Q_- |D|^2), \\ H_V &= \left\{ 2 [Q_+ |C_1|^2 + Q_- |D_1|^2] + \frac{2}{3} \left[Q_+ \left| C_1 - \frac{Q_-}{m_f} C_2 \right|^2 + Q_- \left| D_1 - \frac{Q_+}{m_f} D_2 \right|^2 \right] \right. \\ &\quad + \frac{1}{3m_f^2 q^2} \left[Q_+ \left| (M_+ M_- - q^2) C_1 + Q_- M_+ C_2 + \frac{Q_+ Q_-}{2} C_3 \right|^2 \right. \\ &\quad \left. \left. + Q_- \left| (M_+ M_- - q^2) D_1 - Q_+ M_- D_2 + \frac{Q_+ Q_-}{2} D_3 \right|^2 \right] \right\}. \end{aligned} \quad (7)$$

In Eq. (6), the momentum p_c is given by $p_c = \frac{1}{2m_i} \lambda^{1/2}(m_i^2, m_f^2, q^2)$, where the Källén function is defined as $\lambda(x, y, z) = x^2 + y^2 + z^2 - 2xy - 2xz - 2yz$. For two-body decays, the on-shell condition $q^2 = m_{P,V}^2$ applies, making p_c a constant determined by the masses of the initial and final baryons. The other related notations in Eq. (7) are given as $M_{\pm} = m_i \pm m_f$ and $Q_{\pm} = M_{\pm}^2 - q^2$. Evidently, H_M depends on both the baryon and meson in the final state.

B. Semi-leptonic decays

The decay width of semi-leptonic decays can be generally written as

$$\Gamma(\mathcal{B}_i \rightarrow \mathcal{B}_f \ell^+ \nu_\ell) = \frac{1}{192\pi^3 m_i^2} \int_{m_\ell^2}^{(m_i - m_f)^2} \frac{(q^2 - m_\ell^2)^2 p_c}{q^2} H_\ell dq^2, \quad (8)$$

$$H_\ell = \left(1 + \frac{m_\ell^2}{2q^2}\right) b_V H_V + \frac{3m_\ell^2}{2q^2} b_P H_P,$$

where p_c is not a constant due to the off-shell lepton pair momentum transfer q^2 in three-body decays. As a key component of the phase space integral, H_ℓ can be divided into vector and scalar parts, denoted as H_V and H_P (or H_M in general), with corresponding coefficients

$$b_M = \frac{2}{|V_{ud}|^2 a_1^2 f_M^2 m_M^2}, \quad (M = P, V). \quad (9)$$

It is worth mentioning that the coefficient b_M establishes a connection between hadronic decay and semi-leptonic decay by removing the meson information from H_M defined in Eq. (7), including the meson decay constant f_M and effective Wilson coefficient a_1 (or a_2), introduced in Cabibbo-favored non-leptonic decay processes.

C. The parameterization of amplitudes and form factors

It is widely accepted that both factorizable and non-factorizable amplitudes contribute to general charmed baryon decay processes. In the special case where the decay amplitude only receives factorizable contributions, the partial wave amplitudes can be expressed in terms of form factors and the decay constant, giving

$$\begin{aligned} C &= -\lambda a_1 f_P [\bar{g}_1(m_P^2) + (m_i - m_f) \bar{g}_2(m_P^2) + (m_i E_f - m_f^2) \bar{g}_3(m_P^2)], \\ D &= \lambda a_1 f_P [\bar{f}_1(m_P^2) - (m_i + m_f) \bar{f}_2(m_P^2) + (m_i E_f - m_f^2) \bar{f}_3(m_P^2)], \\ C_i &= -\lambda a_1 f_V m_V \bar{g}_i(m_V^2), \\ D_i &= \lambda a_1 f_V m_V \bar{f}_i(m_V^2), \end{aligned} \quad (10)$$

which depend on the form factors and the meson decay constant $f_M(M = P, V)$ defined as

$$\begin{aligned}\langle 0|\bar{q}_1\gamma_\mu\gamma_5q_2|P(p)\rangle &= ip_\mu f_P, \\ \langle 0|\bar{q}_1\gamma_\mu q_2|V(\lambda)\rangle &= m_V f_V \epsilon_\mu^\lambda.\end{aligned}\tag{11}$$

For the focused $\Omega_c \rightarrow \Omega^-$ process in this work, the effective Wilson coefficient is a_1 while the CKM factor is defined as $\lambda = \frac{G_F}{\sqrt{2}}V_{cs}V_{ud}^*$, together with the final baryon energy $E_f = \frac{m_i^2 + m_f^2 - m_M^2}{2m_i}$. There are several different conventions for related baryon transition form factors, although physical observables are independent of form factor parameterization. In this work, the form factors are parameterized as

$$\begin{aligned}\langle \mathcal{B}_f(p_f)|V_\mu - A_\mu|\mathcal{B}_i(p_i)\rangle &= \bar{u}_f' [(\bar{f}_1(q^2)g_{\nu\mu} + \bar{f}_2(q^2)p_{i\nu}\gamma_\mu + \bar{f}_3(q^2)p_{i\nu}p_{f\mu})\gamma_5 \\ &\quad - (\bar{g}_1(q^2)g_{\nu\mu} + \bar{g}_2(q^2)p_{i\nu}\gamma_\mu + \bar{g}_3(q^2)p_{i\nu}p_{f\mu})] u_i,\end{aligned}\tag{12}$$

with the same convention as in [7]. In Appendix A, we summarize different conventions and provide correspondences among them.

III. FORM FACTORS IN THE QUARK MODEL

In this section, we comprehensively investigate non-perturbative $\frac{1}{2}^+ \rightarrow \frac{3}{2}^+$ baryon transition form factors within the non-relativistic constituent quark model to incorporate several types of decays consistently. To describe a spin- $\frac{3}{2}$ particle in the final state, we introduce the Rarita-Schwinger vector spinor u^μ [7, 26]. Its components for $\frac{3}{2}$, $\frac{1}{2}$, $-\frac{1}{2}$, and $-\frac{3}{2}$ spins are given by:

$$\begin{aligned}u_1^\mu &= (0, \vec{\epsilon}_1 u_\uparrow), \\ u_2^\mu &= \left(\sqrt{\frac{2}{3}} \frac{|\vec{p}|}{m} u_\uparrow, \frac{1}{\sqrt{3}} \vec{\epsilon}_1 u_\downarrow - \sqrt{\frac{2}{3}} \frac{E}{m} \vec{\epsilon}_3 u_\uparrow \right), \\ u_3^\mu &= \left(\sqrt{\frac{2}{3}} \frac{|\vec{p}|}{m} u_\downarrow, \frac{1}{\sqrt{3}} \vec{\epsilon}_2 u_\uparrow - \sqrt{\frac{2}{3}} \frac{E}{m} \vec{\epsilon}_3 u_\downarrow \right), \\ u_4^\mu &= (0, \vec{\epsilon}_2 u_\downarrow),\end{aligned}\tag{13}$$

where \vec{p} is the momentum of the final state baryon along its z -axis, $\vec{\epsilon}_i$ are polarized vectors, and u is the spinor for a spin- $\frac{1}{2}$ particle, giving

$$\vec{\epsilon}_1 = \frac{1}{\sqrt{2}} \begin{pmatrix} 1 \\ i \\ 0 \end{pmatrix}, \quad \vec{\epsilon}_2 = \frac{1}{\sqrt{2}} \begin{pmatrix} 1 \\ -i \\ 0 \end{pmatrix}, \quad \vec{\epsilon}_3 = \frac{1}{\sqrt{2}} \begin{pmatrix} 0 \\ 0 \\ 1 \end{pmatrix}; \quad u(p) = \begin{pmatrix} 1 \\ \frac{\vec{\sigma} \cdot \vec{p}}{E+m} \end{pmatrix} \chi, \tag{14}$$

with the two-component Pauli spinor χ denoting spin up and down. In the rest frame of the parent baryon, the vanishing momentum of the initial particle implies the null lower component of u_i , while we have the relation $\vec{p}_f = -\vec{q}$ in the lower component of u_f .

Now with explicit spinors, after expanding the right-handed side of 6 typical independent equations, among all the 64 ones in the form factor definition Eq. (12), we obtain

$$\begin{aligned}
\langle \mathcal{B}_f(1/2) | V_0 | \mathcal{B}_i(1/2) \rangle &= \sqrt{\frac{2}{3}} \frac{|\vec{p}_f|^2}{m_f} \left[-\frac{1}{2m_f} \bar{f}_1 + \frac{m_i}{2m_f} \bar{f}_2 - \frac{m_i}{2} \bar{f}_3 \right] \\
\langle \mathcal{B}_f(1/2) | A_0 | \mathcal{B}_i(1/2) \rangle &= \sqrt{\frac{2}{3}} \frac{|\vec{p}_f|}{m_f} [\bar{g}_1 + \bar{g}_2 m_i + \bar{g}_3 m_i m_f] \\
\langle \mathcal{B}_f(3/2) | V_x | \mathcal{B}_i(1/2) \rangle &= \frac{|\vec{p}_f|}{\sqrt{2}} \frac{1}{2m_f} \bar{f}_1 \\
\langle \mathcal{B}_f(3/2) | A_x | \mathcal{B}_i(1/2) \rangle &= -\frac{1}{\sqrt{2}} \bar{g}_1 \\
\langle \mathcal{B}_f(1/2) | V_x | \mathcal{B}_i(-1/2) \rangle &= \frac{|\vec{p}_f|}{\sqrt{6}} \frac{1}{(2m_f)} \bar{f}_1 + \sqrt{\frac{2}{3}} \frac{|\vec{p}_f| m_i}{m_f} \bar{f}_2 \\
\langle \mathcal{B}_f(1/2) | A_x | \mathcal{B}_i(-1/2) \rangle &= -\bar{g}_1 \frac{1}{\sqrt{6}} + \sqrt{\frac{2}{3}} \frac{|\vec{p}_f|^2 m_i}{2m_f^2} \bar{g}_2
\end{aligned} \tag{15}$$

by choosing the x component of the (axial-)vector part.

Evidently, the six form factors can be expressed as combinations of the non-perturbative matrix elements on the left-hand side of Eq. (15). We will investigate these non-perturbative parameters within the framework of the nonrelativistic constituent quark model to quantitatively understand the dynamics, given the absence of first-principle calculations. Utilizing the baryon wave function outlined in [25], a straightforward calculation, detailed in Appendix B, yields

$$\begin{aligned}
\langle \mathcal{B}_f(1/2) | V_0 | \mathcal{B}_i(1/2) \rangle &= N(I) |_{(\frac{1}{2}, \frac{1}{2})} I_H, & \langle \mathcal{B}_f(1/2) | A_0 | \mathcal{B}_i(1/2) \rangle &= \frac{|\vec{p}_f|}{2m_f} N(\sigma_z) |_{(\frac{1}{2}, \frac{1}{2})} Z, \\
\langle \mathcal{B}_f(3/2) | V_x | \mathcal{B}_i(1/2) \rangle &= \frac{|\vec{p}_f|}{2m_f} N(\sigma_x) |_{(\frac{3}{2}, \frac{1}{2})} X, & \langle \mathcal{B}_f(3/2) | A_x | \mathcal{B}_i(1/2) \rangle &= N(\sigma_x) |_{(\frac{3}{2}, \frac{1}{2})} I_H, \\
\langle \mathcal{B}_f(1/2) | V_x | \mathcal{B}_i(-1/2) \rangle &= \frac{|\vec{p}_f|}{2m_f} N(\sigma_x) |_{(\frac{1}{2}, -\frac{1}{2})} X, \\
\langle \mathcal{B}_f(1/2) | A_x | \mathcal{B}_i(-1/2) \rangle &= N(\sigma_x) |_{(\frac{1}{2}, -\frac{1}{2})} (I_H - \frac{|\vec{p}_f|^2}{2m_f^2} Y),
\end{aligned} \tag{16}$$

in which the spin-flavor factors $N(A) |_{(s_f, s_i)}$ ($A = I, \sigma_x$) are evaluated to be

$$\begin{aligned}
N(I) |_{(\frac{1}{2}, \frac{1}{2})} &= 0, & N(\sigma_z) |_{(\frac{1}{2}, \frac{1}{2})} &= \frac{-2\sqrt{2}}{3}, \\
N(\sigma_x) |_{(\frac{3}{2}, \frac{1}{2})} &= \sqrt{\frac{2}{3}}, & N(\sigma_x) |_{(\frac{1}{2}, -\frac{1}{2})} &= \frac{\sqrt{2}}{3},
\end{aligned} \tag{17}$$

with particular third-component spin of initial baryon s_i and final s_f , and the auxiliary functions X, Y, Z, Z', I_H given as

$$\begin{aligned}
X &= I_H \left[1 + \frac{2m\alpha_{\lambda_f}^2}{m_q(\alpha_{\lambda_i}^2 + \alpha_{\lambda_f}^2)} + \frac{2m\alpha_{\lambda_i}^2}{m_Q(\alpha_{\lambda_i}^2 + \alpha_{\lambda_f}^2)} \right], \\
Y &= -I_H \left[\frac{2m^2\alpha_{\lambda_i}^4}{m_q m_Q (\alpha_{\lambda_i}^2 + \alpha_{\lambda_f}^2)^2} + \frac{m\alpha_{\lambda_i}^2}{(\alpha_{\lambda_i}^2 + \alpha_{\lambda_f}^2)m_Q} \right], \\
Z &= I_H \left[1 + \frac{2m\alpha_{\lambda_f}^2}{m_q(\alpha_{\lambda_i}^2 + \alpha_{\lambda_f}^2)} - \frac{2m\alpha_{\lambda_i}^2}{m_Q(\alpha_{\lambda_i}^2 + \alpha_{\lambda_f}^2)} \right], \\
Z' &= Z - Y - 2I_H, \\
I_H &= \left(\frac{2\alpha_{\lambda_i}\alpha_{\lambda_f}}{(\alpha_{\lambda_i}^2 + \alpha_{\lambda_f}^2)} \right)^{3/2} \exp \left[\frac{2m^2|\vec{q}|^2}{m_f(\alpha_{\lambda_i}^2 + \alpha_{\lambda_f}^2)} \right],
\end{aligned} \tag{18}$$

originate from integrals of baryon spatial wave functions, which are consistent with the general form given in [27]. These explicit spatial integrals, which were absent from the earlier work [7], reveal the underlying dynamics of baryons. The two types of parameters on which the spatial integrals rely are masses (heavy (light) quark mass m_Q (m_q) involving weak interaction, spectator quark mass m and final baryon mass m_f) and harmonic oscillator parameter α_λ (α_ρ depends on α_λ ; α_{λ_i} (α_{λ_f}) stands for initial (final) baryon parameter). In this work, the naturally accommodated condition $\alpha_{\rho i} = \alpha_{\rho f}$, due to the identical ρ -mode shared by the initial particle Ω_c and final particle Ω, Ξ^- , further simplifies Eq. (18) and hence leads to a cancellation of α_ρ dependence.¹

In the zero recoil limit ($q^2 = q_{\text{max}}^2$), the FFs can be solved combining Eq. (15) and (18), giving

$$\begin{aligned}
\bar{f}_1 &= \frac{2}{\sqrt{3}}X, & \bar{f}_2 &= \frac{1}{\sqrt{3}m_i}X, & \bar{f}_3 &= \frac{-1}{\sqrt{3}m_i m_f}X \\
\bar{g}_1 &= -\frac{2}{\sqrt{3}}I_H, & \bar{g}_2 &= -\frac{1}{\sqrt{3}m_i}Y, & \bar{g}_3 &= -\frac{Z'}{\sqrt{3}m_i m_f},
\end{aligned} \tag{19}$$

with \mathcal{B}_i (\mathcal{B}_f) mass m_i (m_f) and the three-momentum $|\vec{q}| = 0$. Specifically, the uncertainties in all six form factors, and consequently in the factorizable amplitudes, arise solely from quark masses, owing to the cancellation involving α_ρ in the ratios shown in Eq. (18). In our practical calculation, we need the evolutions of form factors with respect to q^2 to estimate physical observables. In this work, we follow the parametrization [28]

$$f_i(q^2) = \frac{f_i(0)}{(1 - q^2/m_V^2)^2}, \quad g_i(q^2) = \frac{g_i(0)}{(1 - q^2/m_A^2)^2}, \tag{20}$$

adopted in our previous series of works [15–19, 24, 25] to capture the typical evolution behaviors, in which the pole masses are taken as $m_V = 2.11$ GeV, $m_A = 2.54$ GeV.

¹ The relation between λ -mode and ρ -mode presented as Eq. (21) is also taken into account.

TABLE II. Input parameters adopted in this work. Parameters listed in the upper entries without a reference are taken from PDG [22], while those in the lower entries are from [29]^a.

Parameters	Values	Parameters	Values
$m_{\Omega_c^0}$	2.695 GeV	m_{Ω^-}	1.672 GeV
m_{Ξ^0}	1.314 GeV	m_{Ξ^-}	1.321 GeV
a_1	1.257 [15]	$\tau_{\Omega_c^0}$	(268 ± 26) fs[30]
V_{cs}	0.9735	V_{ud}	0.9743
V_{cd}	-0.221	V_{us}	0.2251
f_π	130.4(2) MeV [31]	f_ρ	216 MeV [32]
m_u	(0.33 ± 0.05) GeV	m_d	(0.33 ± 0.05) GeV
m_s	(0.45 ± 0.05) GeV	m_c	(1.48 ± 0.10) GeV
α_ρ	(0.325 ± 0.025) GeV ^b		

^a The central values are quoted from [29], while uncertainties here are imposed for illustration of error analysis.

^b Due to the difference in definition conventions, the value adopted here is smaller by a factor of $\sqrt{2}$ compared with the one defined in [29], where $\alpha_\rho = 0.44$ GeV. The slight deviation in central value can be accounted by the imposed error.

IV. NUMERICAL RESULTS AND DISCUSSIONS

Before delving into detailed numerical calculations, interpreting the results, and discussing input sensitivities, we first summarize the input parameters utilized in the following analyses, presented in Table II. Broadly categorized, these input parameters fall into two groups based on their sensitivity to the quark model. The first group comprises parameters that are largely physical, already determined either by experimental measurements or theoretical calculations. These include the masses and lifetimes of baryons, CKM matrix elements, and effective Wilson coefficients. Notably, the effective Wilson coefficient employed in this study is set to $a_1 = 1.257$, determined by fixing $N_{\text{eff}} \approx 7$ as extracted from $\Lambda_c \rightarrow p\phi$ [15, 33]. The second group consists of parameters such as quark masses and the harmonic oscillator parameter α_ρ , which are model-dependent. In the context of the constituent quark model, the central values of light quark masses are chosen as $m_u = m_d = m_l = 0.33$ GeV, while the masses of strange and charm quarks are assigned as 0.45 GeV and 1.48 GeV, respectively [29].

For each baryon, it appears that two harmonic oscillator parameters, α_ρ and α_λ , are required

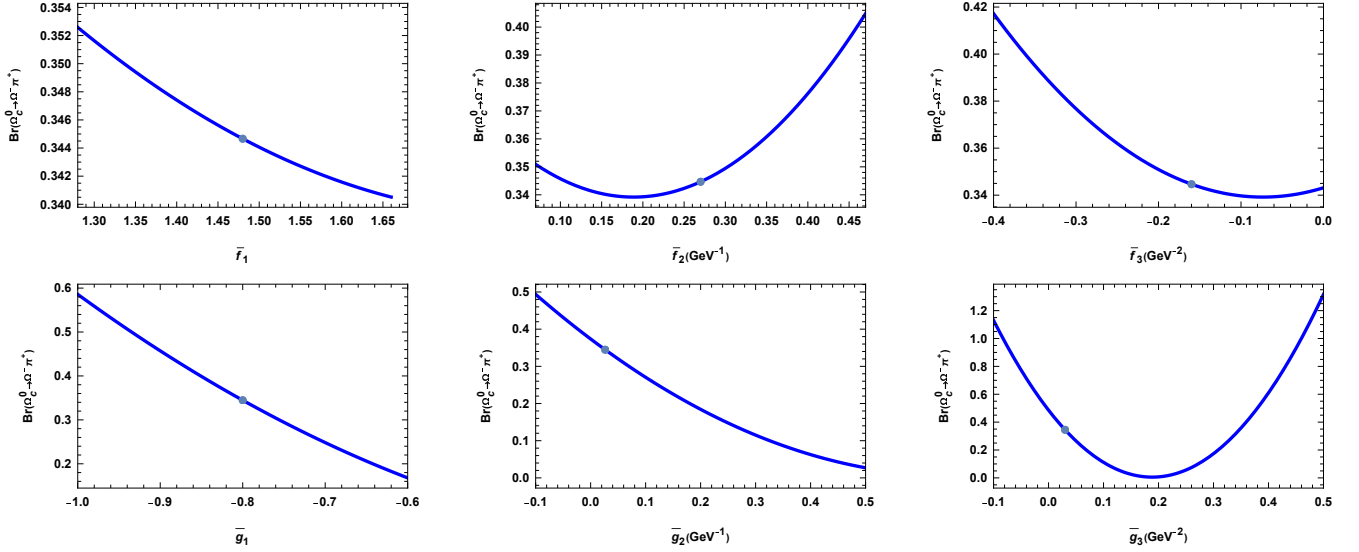


FIG. 1. The form factor dependence of branching fraction for the decay $\Omega_c \rightarrow \Omega^- \pi^+$.

to describe its corresponding excited mode. However, as illustrated in [25], these two strength parameters are interconnected via

$$\alpha_\lambda = \left[\frac{4m_3(m_1 + m_2)^2}{3m_1m_2(m_1 + m_2 + m_3)} \right]^{\frac{1}{4}} \alpha_\rho, \quad (21)$$

where the paired quarks $q_{1,2}$ correspond to their masses $m_{1,2}$, resulting in only one independent oscillator strength for each baryon. Since the baryons Ω_c , Ω , and $\Xi^{0,-}$ share the same ρ -mode, consisting of a pair of strange quarks, it is reasonable to use the relation $\alpha_\rho(\Omega_c) = \alpha_\rho(\Omega) = \alpha_\rho(\Xi^{0,-})$. The fact that $\alpha_{\rho_i} = \alpha_{\rho_f}$ and $\alpha_{\lambda_i} = [(2m_s + m_c)/(3m_c)]^{1/4} \alpha_{\lambda_f}$ simplifies our analysis by reducing the number of free parameters to one, α_ρ , for all processes discussed in this work. In the subsequent numerical evaluations, we adopt the value (0.325 ± 0.025) GeV for α_ρ [29], leading to $\alpha_\lambda(\Omega_c^0) = (0.438 \pm 0.034)$ GeV, $\alpha_\lambda(\Omega^-) = (0.375 \pm 0.029)$ GeV, and $\alpha_\lambda(\Xi^0, \Xi^-) = (0.355 \pm 0.027)$ GeV. All the inputs relevant to the numerical analyses in this work are presented in Table II.

A. Form factors

The decay mode $\Omega_c \rightarrow \Omega^- \pi^+$ holds significant importance in experiments as it serves as a benchmark mode. Moreover, this channel holds a special place in theory as it receives pure factorizable contributions, relying on the $\Omega_c \rightarrow \Omega^-$ transition form factors. Before delving into the detailed dynamics of these form factors, a preliminary examination of their impact on the branching fraction proves beneficial. It is understood that in $\frac{1}{2}^+ \rightarrow \frac{1}{2}^+$ decays, the branching fractions are predominantly governed by f_1 and g_1 , while the contributions from the others can be

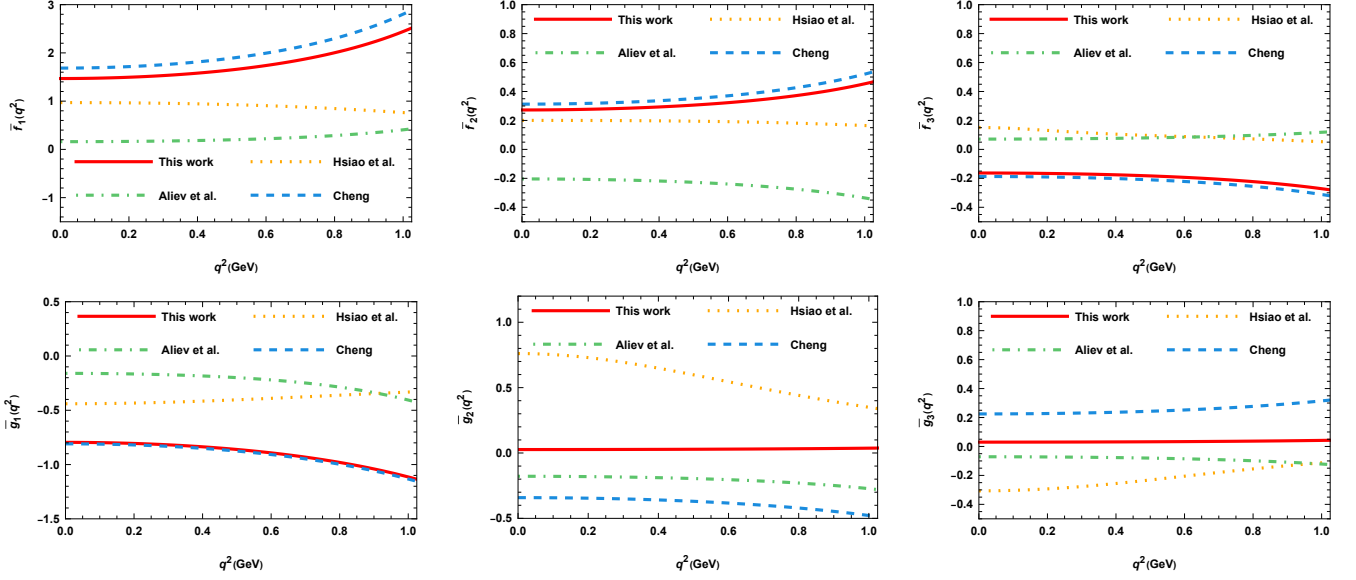


FIG. 2. The evolution of form factors compare with several methodologies, including the early NRQM [7], light cone sum rules [12] and light-front quark model [9].

overlooked. However, in the case of $\frac{1}{2}^+ \rightarrow \frac{3}{2}^+$ transitions, each form factor contributes significantly. In each plot of Fig. 1, marked by the point at the physical scale, although the individual behaviors vary, the contributions to the branching fraction from all 6 form factors are of a similar magnitude.

In the context of the non-relativistic constituent quark model, we illustrate the individual behaviors of the 6 form factors of the $\Omega_c^0 \rightarrow \Omega^-$ process in Fig. 2, which primarily depend on the constituent quark mass and the harmonic oscillator strength α_ρ . Among the 6 form factors, \bar{f}_1 , \bar{f}_2 , \bar{g}_2 , and \bar{g}_3 exhibit positive values, while \bar{f}_3 and \bar{g}_1 are negative. The predicted behaviors presented by other groups, with convention transferred, are also included for comparison. Although the real integral of the spatial wave function was not considered in the previous non-relativistic quark model calculation [7], our results demonstrate consistent and similar behaviors for \bar{f}_1 , \bar{f}_2 , \bar{f}_3 , and \bar{g}_1 . The discrepancies are more apparent when comparing our results with calculations from the light-cone sum rule [12] and the light-front quark model [9]. For instance, regarding \bar{f}_1 , our results agree with the light-cone sum rule in terms of evolution behavior but differ in size. In contrast, when comparing with the light-front quark model prediction, the size difference is up to two times, while the evolution behaviors are opposite. Hence, further scrutiny of these form factors from experimental data or lattice QCD simulations is necessary and anticipated.

B. Branching fractions

Without a clear understanding of the reference mode $\Omega_c \rightarrow \Omega^- \pi^+$, the predictions of other modes lack conviction. Therefore, our top priority here is to provide an explicit numerical prediction for this benchmark channel.

1. The benchmark channel $\Omega_c \rightarrow \Omega^- \pi^+$ and $\Omega_c \rightarrow \Omega^- \rho^+$

The decay mode $\Omega_c \rightarrow \Omega^- \pi^+$ holds special significance as it primarily involves purely factorizable contributions described by baryon transition form factors. By setting up the kinematics for $\frac{1}{2}^+ \rightarrow \frac{3}{2}^+ + 0^-$ and utilizing the analytically calculated form factors $\bar{f}_i(m_P^2)$ and $\bar{g}_i(m_P^2)$, we can compute its branching fraction. Our predicted value of

$$\mathcal{B}(\Omega_c^0 \rightarrow \Omega^- \pi^+) = (3.43 \pm 0.48)\% \quad (22)$$

closely aligns with the early nonrelativistic quark model (NRQM) prediction of 4.19%, but notably exceeds the predictions of other models. Specifically, constituent quark model (CQM) results [11] hover around the percentage range, whereas predictions are even smaller in both the covariant confined quark model (CCQM) [34] and the light-front quark model (LFQM) [9].

The decay $\Omega_c \rightarrow \Omega^- \rho^+$ shares similarities with the benchmark mode, as its amplitude predomi-
TABLE III. Predictions of absolute and relative branching fractions, together with comparisons among different theoretical groups. Only errors for $\Omega_c \rightarrow \Xi^- \pi^+$ has been denoted, originated from its component of non-factorizable contribution.

	This work	Cheng [7]	Wang et al.[11]	Gutsche et al.[34]	Hsiao et al.[9]	Aliev et al.[12]	Liu [13]
$\Omega_c^0 \rightarrow \Omega^- \pi^+$	$(3.43 \pm 0.48)\%$	4.19%	1.1%	0.2%	0.51%	2.9%	1.88%
$\Omega_c^0 \rightarrow \Omega^- \rho^+$	$(18.30 \pm 1.94)\%$	15.08%		1.9%	$1.44 \pm 0.04\%$	6.3%	
$\Omega_c^0 \rightarrow \Xi^- \pi^+$	$(0.54 \pm 0.18)\%$						0.94%
$\Omega_c^0 \rightarrow \Omega^- e^+ \nu_e$	$(4.06 \pm 0.48)\%$				$0.54 \pm 0.02\%$	2.06%	2.54%
$\Omega_c^0 \rightarrow \Omega^- \mu^+ \nu_\mu$	$(3.81 \pm 0.44)\%$				$0.50 \pm 0.02\%$	1.96%	
$R(\Omega^- \rho^+)$	5.33 ± 0.94	3.60		9.5	2.8 ± 0.4	2.18	
$R(\Xi^- \pi^+)$	0.16 ± 0.06						0.5
$R(\Omega^- e^+ \nu_e)$	1.18 ± 0.22				1.1 ± 0.2	0.71	1.35
$R(\Omega^- \mu^+ \nu_\mu)$	1.11 ± 0.20				1.059	0.68	
$R(\Omega^- e^+ \nu_e)/R(\Omega^- \mu^+ \nu_\mu)$	1.07 ± 0.18				1.08	1.04	

TABLE IV. The predicted S - and P -wave amplitude (in units of $10^{-2}G_F^2$ GeV) of $\Omega_c^0 \rightarrow \Xi^- \pi^+$ decay.

	A^{fac}	A^{nf}	A^{tot}	B^{fac}	B^{nf}	B^{tot}	\mathcal{B}
$\Omega_c^0 \rightarrow \Xi^- \pi^+$	-0.950 ± 0.094	-2.233 ± 0.549	-3.183 ± 0.557	-1.493 ± 0.150	1.481 ± 0.343	-0.012 ± 0.373	$(0.535 \pm 0.179)\%$

nantly consists of purely factorizable contributions. However, the kinematics are more complicated due to the presence of the final vector meson. Despite this complexity, we calculate a branching fraction of 18.39%, which closely resembles the early NRQM prediction of 15.08%, but is approximately an order of magnitude larger than the predictions of CCQM [34] and LFQM [9].

To date, directly measuring the benchmark mode remains challenging. However, some ratios between other modes and the reference mode are available. Notably, only Belle has reported a lower bound of $R(\Omega^- \rho^+) > 1.3$, which aligns with the predictions of all theoretical models.

2. Non-leptonic decay $\Omega_c \rightarrow \Xi^- \pi^+$

The mode $\Omega_c \rightarrow \Xi^- \pi^+$ is a typical non-leptonic decay since it receives both factorizable and non-factorizable contributions. In the framework of topological diagram approach by combining the pole model at hadron level and MIT bag model at quark level, Ω_c decays have been studied systematically in [24]. To reduce the uncertainty of quark model estimation of non-perturbative parameters, it is valuable to investigate them in a separated approach. General speaking, the momentum carried by final state particle in the decays of charm system is with smaller velocity comparing with those decayed from B system, thus a choice of non-relativistic quark model is reasonable. By collecting necessary formulae for factorizable and non-factorizable amplitudes directly from [24]

$$\begin{aligned}
 A^{\text{fac}} &= \frac{G_F}{\sqrt{2}} a_1 V_{ud}^* V_{cd} f_\pi (m_{\Omega_c} - m_{\Xi^-}) f_1, \\
 B^{\text{fac}} &= -\frac{G_F}{\sqrt{2}} a_1 V_{ud}^* V_{cd} f_\pi (m_{\Omega_c} + m_{\Xi^-}) g_1, \\
 A^{\text{nf}} &= \frac{1}{f_\pi} a_{\Xi^0 \Omega_c^0}, \\
 B^{\text{nf}} &= \frac{1}{f_\pi} \left(g_{\Xi^- \Xi^0}^{A(\pi^+)} \frac{m_{\Xi^-} + m_{\Xi^0}}{m_{\Omega_c^0} - m_{\Xi^0}} a_{\Xi^0 \Omega_c^0} \right),
 \end{aligned} \tag{23}$$

and numerically calculating corresponding non-perturbative parameters

$$f_1 = 0.276 \pm 0.028, \quad g_1 = -0.148 \pm 0.015, \quad g_{\Xi^- \Xi^0}^{A(\pi^+)} = -0.334 \pm 0.044, \quad a_{\Xi^0 \Omega_c^0} = (-3.148 \pm 0.715) \times 10^{-3} \tag{24}$$

we predict its branching fraction as

$$\mathcal{B}(\Omega_c \rightarrow \Xi^- \pi^+) = (5.35 \pm 1.79) \times 10^{-3}. \quad (25)$$

For the α_ρ cancellation in FFs, the dominated error originated from oscillator parameter only affects non-factorizable contribution. Therefore only the errors of four-quark operator matrix element and hence branching fraction have been calculated. Compared with our previous MIT bag model calculation, in which $f_1 = 0.25, g_1 = -0.12, g_{\Xi^- \Xi^0}^{A(\pi^+)} = -0.217, a_{\Xi^0 \Omega_c} = -4.54 \times 10^{-4}$, and hence $\mathcal{B}(\Omega_c \rightarrow \Xi^- \pi^+) = 9.34 \times 10^{-3}$ [24], the decrease of branching fraction is mainly due to an enhancement of matrix element of four-quark operator $a_{\Xi^0 \Omega_c}$. Similar enhancement of matrix element, and hence enhancement of non-factorizable contribution, was also observed in the study of decay of doubly charmed baryon decays [25], by comparing MIT bag model and NR constitute quark model. We display the contributed components of $\Omega_c \rightarrow \Xi^- \pi^+$ in Table IV for more details. Although it is still challenging to give a direct measurement of such a decay, the calculated relative ratio

$$R(\Xi^- \pi^+) = 0.156 \pm 0.057 \quad (26)$$

is consistent well with the recent measured value 0.158 ± 0.011 reported by LHCb [5].

3. Semi-leptonic decays $\Omega_c \rightarrow \Omega^- \ell^+ \nu_\ell$

For the semi-leptonic decay, the leptons in the final state is specific to electron and muon. Obviously in the massless limit of leptons, the branching fraction is identical since it only receives contribution from H_V according to Eq. (8). In practice, the lepton mass effect accounts, leading to close but slightly deviated branching fractions for $\Omega_c \rightarrow \Omega^- e^+ \nu_e$ and $\Omega_c \rightarrow \Omega^- \mu^+ \nu_\mu$. With the prepared FFs \bar{f}_i and \bar{g}_i , the branching fractions of semi-leptonic decays are calculated to be

$$\mathcal{B}(\Omega_c \rightarrow \Omega^- e^+ \nu_e) = (4.06 \pm 0.48)\%, \quad \mathcal{B}(\Omega_c \rightarrow \Omega^- \mu^+ \nu_\mu) = (3.81 \pm 0.44)\%, \quad (27)$$

which are around one order of magnitude larger than the predictions in [9] and twice larger than calculation in light-cone sum rule [12]. Although so far no direct discrimination from experiment is available, the relative ratios to reference mode can still provide supportive information. Results in our calculation,

$$R(\Omega^- e^+ \nu_e) = 1.18 \pm 0.22, \quad R(\Omega^- \mu^+ \nu_\mu) = 1.11 \pm 0.20, \quad (28)$$

are slight smaller than [13], close to the one obtained in [9], but quite larger than [12] among the theoretical groups. Our predictions, On the other hand, though are smaller than Belle measurement $R(\Omega^- e^+ \nu_e) = 1.98 \pm 0.15$, $R(\Omega^- \mu^+ \nu_\mu) = 1.94 \pm 0.21$, are consistent with recent ALICE reported value $R(\Omega^- e^+ \nu_e) = 1.12 \pm 0.35$. A further discrimination by more precise measurement in experiment or calculation from first principle in theory is thus highly anticipated.

V. CONCLUDING REMARKS

Inspired by the recent LHCb and ALICE measurement of Ω_c decays, we study its semi-leptonic and non-leptonic decay processes in this work. Our main results are as follows.

- Branching fractions of $\Omega_c \rightarrow \Omega P$, $\Omega_c \rightarrow \Omega V$ and $\Omega_c \rightarrow \Omega \ell^+ \nu_\ell$ all receive contributions from $\frac{1}{2}^+ \rightarrow \frac{3}{2}^+$ transition form factors. Conventions of these FFs are unified. Unlike $\frac{1}{2}^+ \rightarrow \frac{1}{2}^+$ decays, in which f_1 and g_1 give dominated contributions to branching fraction, all the 6 FFs provide comparable components to the branching fraction as displayed in Fig. 1.
- In the framework of NRQM, we performed an analytical calculation of 6 FFs related to $\Omega_c^0 \rightarrow \Omega^-$. It is interesting to note that all the FFs depends only on constitute quark masses and one oscillation parameter α_ρ . We make a comparison with other groups for the estimation of FFs numerically. As shown in Fig. 2, deviations exist among different methods and further scrutiny is required in the future.
- We estimated absolute and relative branching fractions of types of decays, including benchmark mode $\Omega_c^0 \rightarrow \Omega^- \pi^+$, $\Omega_c^0 \rightarrow \Omega^- \rho^+$, $\Omega_c^0 \rightarrow \Xi^- \pi^+$, $\Omega_c^0 \rightarrow \Omega^- e^+ \nu_e$ and $\Omega_c^0 \rightarrow \Omega^- \mu^+ \nu_\mu$. The results are presented in Table III.
- Although the above absolute branching fractions can not be measured directly, some of their relative ratios to benchmark mode have been measured recently. Within NRQM and taking quark mass and oscillator parameter α_ρ as inputs, our predictions generally satisfy all the current available experimental data. Especially, our prediction of $R(\Xi^- \pi^+)$ agrees well with the recent LHCb 2023 measurement for the first time, which is evident from a combination of Table I and III. For the semi-leptonic decays, although the prediction of $R(\Omega^- e^+ \nu_e)$ and $R(\Omega^- \mu^+ \nu_\mu)$ in this work has more than 5σ deviation from Belle 2022 result, it is consistent well with recent result reported by ALICE 2024.

The study of Ω_c offers valuable insights into charmed baryon physics and opens up new opportunities to explore the dynamics at the charm scale. Further developments on Ω_c both in experiment and theory, including first principle calculation from Lattice QCD, are highly anticipated.

Note Added

All the authors contribute equally and they are co-first authors, while F. Xu is the corresponding author.

ACKNOWLEDGMENTS

We would like to thank Hai-Yang Cheng, Xiao-Rui Lyu, Jin-Lin Fu and Feng-Zhi Chen for valuable discussions. This research is supported by the National Natural Science Foundation of China under Grant Nos. 12475095 and U1932104.

Appendix A: Conventions of form factors

For the baryon decay $\frac{1}{2}^+ \rightarrow \frac{3}{2}^+$, generically there are 8 form factors to describe the baryon transition under the $V - A$ current. One parameterization, see [34, 35], is taken as

$$\begin{aligned} \langle \mathcal{B}_f(p_f) | V_\mu - A_\mu | \mathcal{B}_i(p_i) \rangle = \bar{u}_f^\nu & \left[\left(F_1(q^2) g_{\nu\mu} + F_2(q^2) \frac{p_{i\nu}}{m_i} \gamma_\mu + F_3(q^2) \frac{p_{i\nu} p_{f\mu}}{m_i^2} + F_4(q^2) \frac{p_{i\nu} q_\mu}{m_i^2} \right) \gamma_5 \right. \\ & \left. - \left(G_1(q^2) g_{\nu\mu} + G_2(q^2) \frac{p_{i\nu}}{m_i} \gamma_\mu + G_3(q^2) \frac{p_{i\nu} p_{f\mu}}{m_i^2} + G_4(q^2) \frac{p_{i\nu} q_\mu}{m_i^2} \right) \right] u_i. \end{aligned} \quad (\text{A1})$$

The (axial-)vector current form factor F_j (G_j) ($j = 1, 2, 3, 4$) depends on momentum transfer q^2 , and q is defined as $q = p_i - p_f$. In our work, we take a convention with 6 independent form factors (see Eq. (12)) which was adopted in [7]. In fact, by making use of the following relations,

$$\begin{aligned} \bar{f}_1 = F_1, \quad \bar{f}_2 = \frac{F_2}{m_i}, \quad p_{f\mu} \bar{f}_3 = \frac{p_{f\mu} F_3 + q_\mu F_4}{m_i^2} \\ \bar{g}_1 = G_1, \quad \bar{g}_2 = \frac{G_2}{m_i}, \quad p_{f\mu} \bar{g}_3 = \frac{p_{f\mu} G_3 + q_\mu G_4}{m_i^2}. \end{aligned} \quad (\text{A2})$$

one may easily understand the two parameterizations are equivalent.

Here we display the difference and connection between parameterizations of FFs in terms of Eq. (A1) and Eq. (12). Whether to incorporate F_4 and G_4 is the main crux. Since they do not enter

the contributed amplitudes of modes decaying into vector meson in view of helicity amplitudes [34], we only need to consider decays of $\frac{1}{2}^+ \rightarrow \frac{3}{2}^+ + 0^-$. Taking the D term of Eq. (10) as an example, with the help of relation $q \cdot p_f = \frac{1}{2}(m_i^2 - m_f^2 - q^2) = (m_i E_f - m_f^2)$ by incorporating on-shell condition $q^2 = m_P^2$, we have

$$\begin{aligned}
D &= \lambda a_1 f_P [\bar{f}_1 - (m_i + m_f) \bar{f}_2 + (m_i E_f - m_f^2) \bar{f}_3] \\
&= \lambda a_1 f_P \left[F_1 - \frac{m_i + m_f}{m_i} F_2 + \frac{p_f \cdot q F_3 + q^2 F_4}{m_i^2} \right] \\
&= \lambda a_1 f_P \left[F_1 - F_2 \frac{m_i + m_f}{m_i} + F_3 \frac{m_i^2 - m_f^2 - q^2}{2m_i^2} + F_4 \frac{q^2}{m_i^2} \right], \tag{A3}
\end{aligned}$$

where the corresponding relation Eq. (A2) has been used in the second equation. Apparently, as contributed components to decay width, our Eq. (10) is equivalent to corresponding terms in Eq. (43) of [34].

There is another set of convention in terms of 8 independent form factors adopted in [9, 12, 27, 36, 37], giving

$$\begin{aligned}
\langle \mathcal{B}_f^*(p_f) | V_\mu - A_\mu | \mathcal{B}_i(p_i) \rangle &= \bar{u}_f^\nu \left[\left(f_1(q^2) \frac{p_{i\nu}}{m_i} \gamma_\mu + f_2(q^2) \frac{p_{i\nu} p_{i\mu}}{m_i^2} + f_3(q^2) \frac{p_{i\nu} p_{f\mu}}{m_i m_f} + f_4(q^2) g_{\nu\mu} \right) \gamma_5 \right. \\
&\quad \left. - \left(g_1(q^2) \frac{p_{i\nu}}{m_i} \gamma_\mu + g_2(q^2) \frac{p_{i\nu} p_{i\mu}}{m_i^2} + g_3(q^2) \frac{p_{i\nu} p_{f\mu}}{m_i m_f} + g_4(q^2) g_{\nu\mu} \right) \right] u_i. \tag{A4}
\end{aligned}$$

By applying the following correspondence

$$\begin{aligned}
\bar{f}_1 &= f_4, & \bar{f}_2 &= \frac{f_1}{m_i}, & \bar{f}_3 &= \frac{(f_2 + f_3)}{m_i m_f}, \\
\bar{g}_1 &= g_4, & \bar{g}_2 &= \frac{g_1}{m_i}, & \bar{g}_3 &= \frac{(g_2 + g_3)}{m_i m_f}, \tag{A5}
\end{aligned}$$

an equivalence to our Eq. (12) can be established.

Appendix B: Model calculations of form factors

Taking \bar{f}_1 as an example, we show necessary details on the calculation of FFs in this section. We shall start from the relations between matrix elements and form factors Eq. (16) at the rest frame of the parent baryon. The quark operator $V_\mu = \bar{q} \gamma_\mu Q$ (or $A_\mu = \bar{q} \gamma_\mu \gamma_5 Q$) will be expanded by two-component Pauli spinor with

$$Q = \begin{pmatrix} 1 \\ \frac{\boldsymbol{\sigma} \cdot \mathbf{p}_Q}{2m_Q} \end{pmatrix} \chi_\pm, \quad \bar{q} = \chi_\pm^\dagger \left(1, \frac{\boldsymbol{\sigma} \cdot \mathbf{p}_q}{2m_q} \right). \tag{B1}$$

To match specific components, we denote \mathbf{p}_Q and \mathbf{p}_q as the momenta of the heavy quark Q and the light quark q , which are involved in the decay $Q \rightarrow q$ at the quark level. These momenta as parts of momenta of the initial and final baryons, satisfying $\mathbf{p}_i - \mathbf{p}_f = \mathbf{p}_Q - \mathbf{p}_q$. In order to extract \bar{f}_1 , we take the spatial component x and spin component $(s_i, s_f) = (\frac{1}{2}, \frac{3}{2})$ in Eq. (16), giving

$$\begin{aligned}
\langle \mathcal{B}_f(3/2) | V_x | \mathcal{B}_i(1/2) \rangle &= \int d\mathbf{p}_{\rho i} d\mathbf{p}_{\lambda i} d\mathbf{p}_{\rho f} d\mathbf{p}_{\lambda f} \Psi_{(\mathbf{p}_{\rho f}, \mathbf{p}_{\lambda f})}^{*3/2} \Psi_{(\mathbf{p}_{\rho i}, \mathbf{p}_{\lambda i})}^{1/2} \langle q'_3 q'_2 q | \bar{q} \gamma_1 Q | Q q_2 q_3 \rangle \\
&= \int d\mathbf{p}_{\rho i} d\mathbf{p}_{\lambda i} d\mathbf{p}_{\rho f} d\mathbf{p}_{\lambda f} \Psi_{(\mathbf{p}_{\rho f}, \mathbf{p}_{\lambda f})}^{*3/2} \Psi_{(\mathbf{p}_{\rho i}, \mathbf{p}_{\lambda i})}^{1/2} \langle q'_3 q'_2 | q_2 q_3 \rangle \langle q | \bar{q} \gamma_1 Q | Q \rangle \\
&= N(\sigma_x) |_{(\frac{3}{2}, \frac{1}{2})} \int d\mathbf{p}_{\rho i} d\mathbf{p}_{\lambda i} d\mathbf{p}_{\rho f} d\mathbf{p}_{\lambda f} \Psi_{(\mathbf{p}_{\rho f}, \mathbf{p}_{\lambda f})}^{*3/2} \left(\frac{\mathbf{p}_q}{2m_q} - \frac{\mathbf{p}_Q}{2m_Q} \right) \Psi_{(\mathbf{p}_{\rho i}, \mathbf{p}_{\lambda i})}^{1/2} \quad (\text{B2}) \\
&\quad \times \delta^3(\mathbf{p}_{\rho i} - \mathbf{p}_{\rho f}) \delta^3\left(\mathbf{p}_{\lambda i} - \mathbf{p}_{\lambda f} - \frac{2m_l}{m_i} \mathbf{p}_f\right) \\
&= \frac{|\vec{p}_f|}{2\sqrt{2}m_f} \bar{f}_1.
\end{aligned}$$

In Eq. (B2), the spin-flavor factor is denoted as $N(\sigma_x) |_{(\frac{3}{2}, \frac{1}{2})}$ and delta functions originate from Jacobi momentum (see [25]). The baryon wave function $\Psi_{(\mathbf{p}_{\rho f}, \mathbf{p}_{\lambda f})}^{3/2}$ and $\Psi_{(\mathbf{p}_{\rho i}, \mathbf{p}_{\lambda i})}^{1/2}$ can be generally expressed in terms of Jacobi momentum \mathbf{p}_ρ and \mathbf{p}_λ

$$\Psi_{N, L, M_L}(\mathbf{P}, \mathbf{p}_\rho, \mathbf{p}_\lambda) = \delta^3(\mathbf{P} - \mathbf{P}_c) \sum_m \langle LM_L | l_\rho m, l_\lambda M_L - m \rangle \psi_{n_\rho l_\rho m}(\mathbf{p}_\rho) \psi_{n_\lambda l_\lambda (M_L - m)}(\mathbf{p}_\lambda), \quad (\text{B3})$$

associated with the quark wave function in momentum space

$$\psi_{nLm}(\mathbf{p}) = (i)^l (-1)^n \left[\frac{2n!}{(n+L+\frac{1}{2})!} \right]^{\frac{1}{2}} \frac{1}{\alpha^{L+\frac{3}{2}}} \exp \left[-\frac{\mathbf{p}^2}{2\alpha^2} \right] L_n^{L+\frac{1}{2}} \left(\frac{\mathbf{p}^2}{\alpha^2} \right) \mathcal{Y}_{Lm}(\mathbf{p}). \quad (\text{B4})$$

For a baryon state with the quantum number $J^P = \frac{3}{2}^+$ in this work, its orbital angular momentum is taken as $L = 0$ to set the parity, yielding the wave function,

$$\Psi_{(\mathbf{p}_{\rho f}, \mathbf{p}_{\lambda f})}^{3/2} = \psi_{000}(\mathbf{p}_{\rho f}) \psi_{000}(\mathbf{p}_{\lambda f}) = \frac{1}{\sqrt{\pi^3}} \frac{1}{(\alpha_{\rho f} \alpha_{\lambda f})^{\frac{3}{2}}} \exp \left[-\frac{1}{2} \left(\frac{\mathbf{p}_{\rho f}^2}{\alpha_{\rho f}^2} + \frac{\mathbf{p}_{\lambda f}^2}{\alpha_{\lambda f}^2} \right) \right], \quad (\text{B5})$$

with only the spin $S = \frac{3}{2}$ component. From the definition of Jacobi momentum, we can derive the two relations $\mathbf{p}_Q = -\mathbf{p}_{\lambda i}$ and $\mathbf{p}_q = -\mathbf{p}_{\lambda i} + \mathbf{p}_f$, which simplify the following calculation, and set \mathbf{p}_f along z -direction in the rest frame of the parent baryon. Combining the explicit wave functions shown in Eq. (B5) and delta function in Eq. (B2), we have

$$\begin{aligned}
\frac{|\vec{p}_f|}{2\sqrt{2}m_f} \bar{f}_1 &= \frac{1}{\pi^3} \frac{1}{(\alpha_{\rho i} \alpha_{\rho f} \alpha_{\lambda i} \alpha_{\lambda f})^{\frac{3}{2}}} N(\sigma_x) |_{(\frac{3}{2}, \frac{1}{2})} \\
&\quad \times \int \left(\frac{-\mathbf{p}_{\lambda i} + |\vec{p}_f|}{2m_q} + \frac{\mathbf{p}_{\lambda i}}{2m_Q} \right) \exp \left[-\frac{1}{2} \left(\frac{\mathbf{p}_{\rho i}^2}{\alpha_{\rho i}^2} + \frac{\mathbf{p}_{\lambda i}^2}{\alpha_{\lambda i}^2} + \frac{\mathbf{p}_{\rho f}^2}{\alpha_{\rho f}^2} + \frac{(\mathbf{p}_{\lambda i} - \frac{2m}{m_f} |\vec{p}_f|)^2}{\alpha_{\lambda f}^2} \right) \right] d\mathbf{p}_{\rho i} d\mathbf{p}_{\lambda i}, \quad (\text{B6})
\end{aligned}$$

with spectator quark mass m , leading to

$$\bar{f}_1 = \frac{2}{\sqrt{3}} \left(\frac{2\alpha_{\lambda_i}\alpha_{\lambda_f}}{\alpha_{\lambda_i}^2 + \alpha_{\lambda_f}^2} \right)^{3/2} \left[1 + \frac{2m\alpha_{\lambda_f}^2}{m_q(\alpha_{\lambda_i}^2 + \alpha_{\lambda_f}^2)} + \frac{2m\alpha_{\lambda_i}^2}{m_Q(\alpha_{\lambda_i}^2 + \alpha_{\lambda_f}^2)} \right]. \quad (\text{B7})$$

Hence the expression of \bar{f}_1 is derived.

-
- [1] A. Zupanc *et al.* [Belle], Phys. Rev. Lett. **113**, no.4, 042002 (2014) doi:10.1103/PhysRevLett.113.042002 [arXiv:1312.7826 [hep-ex]].
- [2] M. Ablikim *et al.* [BESIII], Phys. Rev. Lett. **116**, no.5, 052001 (2016) doi:10.1103/PhysRevLett.116.052001 [arXiv:1511.08380 [hep-ex]].
- [3] Y. B. Li *et al.* [Belle], Phys. Rev. Lett. **122**, no.8, 082001 (2019) doi:10.1103/PhysRevLett.122.082001 [arXiv:1811.09738 [hep-ex]].
- [4] X. Han *et al.* [Belle], JHEP **01** (2023), 055 doi:10.1007/JHEP01(2023)055 [arXiv:2209.08583 [hep-ex]].
- [5] R. Aaij *et al.* [LHCb], Phys. Rev. Lett. **132**, no.8, 081802 (2024) doi:10.1103/PhysRevLett.132.081802 [arXiv:2308.08512 [hep-ex]].
- [6] S. Acharya *et al.* [ALICE], [arXiv:2404.17272 [hep-ex]].
- [7] H. Y. Cheng, Phys. Rev. D **56**, 2799-2811 (1997) [erratum: Phys. Rev. D **99**, no.7, 079901 (2019)] doi:10.1103/PhysRevD.56.2799 [arXiv:hep-ph/9612223 [hep-ph]].
- [8] Q. P. Xu and A. N. Kamal, Phys. Rev. D **46**, 3836-3844 (1992) doi:10.1103/PhysRevD.46.3836
- [9] Y. K. Hsiao, L. Yang, C. C. Lih and S. Y. Tsai, Eur. Phys. J. C **80**, no.11, 1066 (2020) doi:10.1140/epjc/s10052-020-08619-y [arXiv:2009.12752 [hep-ph]].
- [10] Z. X. Zhao, Chin. Phys. C **42**, no.9, 093101 (2018) doi:10.1088/1674-1137/42/9/093101 [arXiv:1803.02292 [hep-ph]].
- [11] K. L. Wang, Q. F. Lü, J. J. Xie and X. H. Zhong, Phys. Rev. D **107**, no.3, 034015 (2023) doi:10.1103/PhysRevD.107.034015 [arXiv:2203.04458 [hep-ph]].
- [12] T. M. Aliev, S. Bilmis and M. Savci, Phys. Rev. D **106**, no.7, 074022 (2022) doi:10.1103/PhysRevD.106.074022 [arXiv:2208.10365 [hep-ph]].
- [13] C. W. Liu, Phys. Rev. D **109**, no.3, 033004 (2024) doi:10.1103/PhysRevD.109.033004 [arXiv:2308.07754 [hep-ph]].
- [14] Y. K. Hsiao, Y. L. Wang and H. J. Zhao, [arXiv:2310.18896 [hep-ph]].

- [15] H. Y. Cheng, X. W. Kang and F. Xu, Phys. Rev. D **97**, no.7, 074028 (2018) doi:10.1103/PhysRevD.97.074028 [arXiv:1801.08625 [hep-ph]].
- [16] J. Zou, F. Xu, G. Meng and H. Y. Cheng, Phys. Rev. D **101**, no.1, 014011 (2020) doi:10.1103/PhysRevD.101.014011 [arXiv:1910.13626 [hep-ph]].
- [17] H. Y. Cheng, G. Meng, F. Xu and J. Zou, Phys. Rev. D **101**, no.3, 034034 (2020) doi:10.1103/PhysRevD.101.034034 [arXiv:2001.04553 [hep-ph]].
- [18] G. Meng, S. M. Y. Wong and F. Xu, JHEP **11**, 126 (2020) doi:10.1007/JHEP11(2020)126 [arXiv:2005.12111 [hep-ph]].
- [19] H. Y. Cheng and F. Xu, Phys. Rev. D **105**, no.9, 094011 (2022) doi:10.1103/PhysRevD.105.094011 [arXiv:2204.03149 [hep-ph]].
- [20] Y. B. Li *et al.* [Belle], Phys. Rev. D **105** (2022) no.9, L091101 doi:10.1103/PhysRevD.105.L091101 [arXiv:2112.10367 [hep-ex]].
- [21] J. Yelton *et al.* [Belle], Phys. Rev. D **97** (2018) no.3, 032001 doi:10.1103/PhysRevD.97.032001 [arXiv:1712.01333 [hep-ex]].
- [22] S. Navas *et al.* (Particle Data Group), to be published in Phys. Rev. D 110, 030001 (2024)
- [23] R. Ammar *et al.* [CLEO], Phys. Rev. Lett. **89** (2002), 171803 doi:10.1103/PhysRevLett.89.171803 [arXiv:hep-ex/0207078 [hep-ex]].
- [24] S. Hu, G. Meng and F. Xu, Phys. Rev. D **101**, no.9, 094033 (2020) doi:10.1103/PhysRevD.101.094033 [arXiv:2003.04705 [hep-ph]].
- [25] S. Zeng, F. Xu, P. Y. Niu and H. Y. Cheng, Phys. Rev. D **107**, no.3, 034009 (2023) doi:10.1103/PhysRevD.107.034009 [arXiv:2212.12983 [hep-ph]].
- [26] D. Lurie, Particles and Fields (Interscience, New York, 1969)
- [27] M. Pervin, W. Roberts and S. Capstick, Phys. Rev. C **74**, 025205 (2006) doi:10.1103/PhysRevC.74.025205 [arXiv:nucl-th/0603061 [nucl-th]].
- [28] Dotcho Fakirov, Berthold Stech Nuclear Physics B, Volume 133, Issue 2,(1978),315-326 doi:10.1016/0550-3213(78)90306-1.
- [29] K. L. Wang, Y. X. Yao, X. H. Zhong and Q. Zhao, Phys. Rev. D **96**, no.11, 116016 (2017) doi:10.1103/PhysRevD.96.116016 [arXiv:1709.04268 [hep-ph]]; K. L. Wang, L. Y. Xiao, X. H. Zhong and Q. Zhao, Phys. Rev. D **95**, no.11, 116010 (2017) doi:10.1103/PhysRevD.95.116010 [arXiv:1703.09130 [hep-ph]].

- [30] R. Aaij *et al.* [LHCb], Phys. Rev. Lett. **121**, no.9, 092003 (2018) doi:10.1103/PhysRevLett.121.092003 [arXiv:1807.02024 [hep-ex]].
- [31] C. Alexandrou *et al.* [Extended Twisted Mass], Phys. Rev. D **104**, no.7, 074520 (2021) doi:10.1103/PhysRevD.104.074520 [arXiv:2104.06747 [hep-lat]].
- [32] P. Maris and P. C. Tandy, Phys. Rev. C **60**, 055214 (1999) doi:10.1103/PhysRevC.60.055214 [arXiv:nucl-th/9905056 [nucl-th]].
- [33] M. Ablikim *et al.* [BESIII], Phys. Rev. Lett. **117**, no.23, 232002 (2016) doi:10.1103/PhysRevLett.117.232002 [arXiv:1608.00407 [hep-ex]].
- [34] T. Gutsche, M. A. Ivanov, J. G. Körner and V. E. Lyubovitskij, Phys. Rev. D **98**, no.7, 074011 (2018) doi:10.1103/PhysRevD.98.074011 [arXiv:1806.11549 [hep-ph]].
- [35] T. Gutsche, M. A. Ivanov, J. G. Körner, V. E. Lyubovitskij and Z. Tyulemissov, Phys. Rev. D **100**, no.11, 114037 (2019) doi:10.1103/PhysRevD.100.114037 [arXiv:1911.10785 [hep-ph]].
- [36] Z. X. Zhao, Eur. Phys. J. C **78**, no.9, 756 (2018) doi:10.1140/epjc/s10052-018-6213-2 [arXiv:1805.10878 [hep-ph]].
- [37] F. Lu, H. W. Ke, X. H. Liu and Y. L. Shi, Eur. Phys. J. C **83**, no.5, 412 (2023) doi:10.1140/epjc/s10052-023-11572-1 [arXiv:2303.02946 [hep-ph]].